

# **Ab Initio Study of Single Pd Atom Functionalized Single-Walled Carbon Nanotubes as Novel Hydrogen Sensing Materials**

*Ling Miao, Venkat R. Bhethanabotla\*, and Babu Joseph*

*Chemical Engineering Department, University of South Florida, Tampa, FL 33620*

Pd functionalized single-walled carbon nanotubes (SWNTs) have recently been used in chemical gas sensor applications. Various functionalized SWNTs have shown great advantages over conventional sensors, in the detection of many types of molecules which are not sensitive to the pristine carbon nanotubes. In this paper, we study the electronic properties of Pd single atom modified SWNTs and their interactions with hydrogen molecules using electronic structure calculations. These calculations were performed using the pseudo-potential plane wave method within density functional theory and the generalized gradient approximation. Two types of SWNTs, armchair tube and zigzag tube, were studied. The interaction between Pd atom and SWNTs leads to a chemisorption bonding involving charge transfer. The electronic structures around Fermi level for both types of tubes were significantly modified. When loaded with H, we have seen a different charge transfer mechanism. The sensing mechanism for hydrogen detection using Pd-SWNT as sensing material will be proposed in detail, and the performance of different type tubes will be further discussed.

## **I. INTRODUCTION**

Single-walled carbon nanotubes (SWNTs)<sup>1</sup> have become some of the most attractive materials for nanodevices because they have special geometries and exhibit many unique electrical and mechanical properties<sup>2,3</sup>. Recently, great advances have been made in applying carbon nanotubes (CNTs) as sensor devices to detect the presence of gases<sup>4,5,6,7-17</sup>, such as O<sub>2</sub>, NH<sub>3</sub>, and NO<sub>2</sub>. The basic principle behind these gas sensors is a change in the electrical conductivity of the semiconducting CNTs, induced by the charge transfer of gas molecules adsorbed on the surfaces. CNTs stand out as an excellent candidate for use as a gas sensing material due to their tendency to change electronic properties at room temperature, as well as the large surface area provided by the center hollow cores and outside walls. For example, sensors fabricated using functionalized SWNTs have shown to be extremely sensitive to the O<sub>2</sub>,<sup>8,9</sup> NH<sub>3</sub>,<sup>9,10</sup> NO<sub>2</sub>,<sup>10,11</sup> or other chemicals<sup>11,12,13</sup>, and biological species,<sup>14,15</sup> by measuring the resistance or conductance of the SWNTs. However, the range of molecules that can be detected by bare CNTs is limited. Gases, such as H<sub>2</sub>, CO, CO<sub>2</sub>, H<sub>2</sub>O and CH<sub>4</sub>, can not be detected. To overcome the limitation of intrinsic CNTs as a sensing material and to offer scope for improving the sensor performance, CNTs are functionalized by several methods, such as substitutional doping,<sup>16</sup> metallic coating,<sup>17,18,19,20</sup> or introduction of functional groups.<sup>21,22</sup> The functionalized CNTs can be characterized by various techniques<sup>23</sup>, like X-ray diffraction, electron spin resonance (ESR)/electron paramagnetic resonance (EPR), ultraviolet (UV)/infrared (IR) spectroscopy, nuclear magnetic resonance (NMR), Raman spectroscopy, etc, and observed by transmission electron microscopy (TEM), atomic force microscopy (AFM) or scanning electron microscopy (SEM). The functionalization of SWNTs induces dramatic changes in both physical and chemical properties of the bare tube, and greatly improves the performance of the sensors.<sup>16-21</sup> One such improvement has been shown on the Pd coated SWNT based hydrogen sensor reported by Kong and co-workers<sup>17</sup>, where a fast response and

high sensitivity and reversibility at room temperature have been observed. Also very recently, Pd loaded SWNTs sensors was tested for CH<sub>4</sub> gas detection.<sup>18</sup> The results show 10 times improvement of sensitivity compared to conventional beads and metal oxide CH<sub>4</sub> sensors. However, even though recent experimental work has shown that functionalized SWNTs achieve a great success on detecting gas molecules, very few theoretical investigations have been made on the gas sensing mechanism of Pd functionalized SWNTs.

In the article, we study the use of Pd functionalized SWNTs as hydrogen gas sensors. Such work is essential to the rational design of novel sensing materials and to achieving a better understanding of the sensing mechanism. In the paper, single Pd atom functionalized SWNTs are considered, *ab initio* pseudo-potential plane-wave calculations within the density functional theory (DFT) are used to obtain the results. Two types of SWNTs are used in this study, semiconducting SWNT(10,0) and metallic SWNT(6,6), with similar diameters of 7.83Å and 8.14Å. SWNT(10,0) is chosen as a typical semiconducting tube because it is dominant in synthesized material.<sup>24</sup> Conducting tube (6,6) is also studied in order to see the potential use of metallic SWNTs in sensors.

## II. COMPUTATIONAL METHODS

The Vienna *ab initio* simulation package (VASP)<sup>25,26,27</sup> was used to perform the periodic system calculations. The total energy and electronic structure calculations are carried out within the generalized gradient approximation (GGA) of PW91<sup>28</sup> using the pseudopotential plane wave method. A large energy cutoff of 500eV for the plane wave basis set is used for all large hexagonal supercells. The SWNTs are considered as isolated and infinite in length, with lateral separation of more than 1nm. To reduce the adatom interactions, supercells are chosen as three times larger than the unit cell in tube direction, namely  $C_{sc} = 2C_{uc}$  for (10,0) tube and  $C_{sc} = 3C_{uc}$  for (6,6) tube. The Brillouin zone of the supercell is sampled by  $1 \times 1 \times 31$  k-points within the Monkhorst-Pack special k-point scheme.<sup>29</sup> Structural configuration of isolated SWNTs and the supercell sizes are fully relaxed to minimize their total energies by conjugate gradient (CG) method. Same sized supercells are used next for adsorption, and all atomic positions of adsorbate and nanotubes are optimized until the remaining forces converge within 0.05eV/Å.

The adsorption,  $E_{ad}$ , for Pd functionalized SWNT is calculated by

$$E_{ad} = E_T(\text{Pd+SWNT}) - E_T(\text{bare SWNT}) - E_T(\text{Pd}),$$

where  $E_T$  is the ground state total energy for different full-relaxed systems. For hydrogen adsorbed on Pd functionalized SWNT system, we apply the similar equation to calculate hydrogen adsorption energy as:

$$E_{ad} = E_T(\text{H+Pd+SWNT}) - E_T(\text{Pd+SWNT}) - E_T(\text{H}).$$

The negative adsorption energies correspond to an energetically bound species.

### III RESULTS and DISCUSSION

#### A. Pd functionalized SWNTs

Four different sites are considered for a single Pd atom functionalized SWNT, as shown in Figure 1. They are top site (above a carbon atom), hollow site (above the center of a carbon ring), and two bridge sites (above the middle of two neighbor carbon atoms), where bridge-1 is perpendicular to the tube axis. Pd adsorbed SWNT system has been reported having a zero magnetic moment<sup>30</sup>, and our calculations of a single Pd atoms also shows the nonmagnetic property. However, we do use spin-polarized DFT in our calculations in the atomic hydrogen + Pd functionalized system in order to observe the possible change of magnetic moment in the interactions of H and Pd.

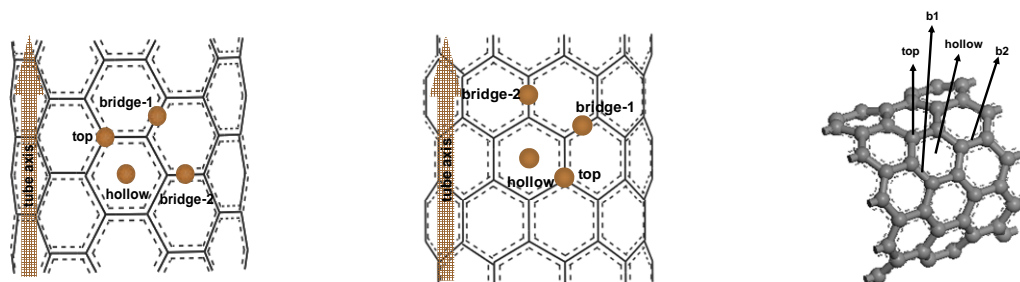


Fig. 1 Schematic drawing of top views of four possible sites for single Pd adsorption on the SWNT(6,6). Brown dots stand for Pd atoms. Bridge-2 site is different from bridge-1 site because the former site located C-C bond is perpendicular to the tube axis. In the SWNT(10,0) case, bridge-2 site is located on a C-C bond paralleling to the tube axis.

**Table 1** Calculated adsorption energies,  $E_{ad}$ , carbon-Pd bond distance  $d_{Pd-C}$ , on different absorption sites on SWNT(6,6), and magnetic moment,  $\mu$ .

System	$E_{ad}$ (eV)	$d_{Pd-C}$ (Å)	$\mu$ ( $\mu_B$ )
Hollow	-0.98	2.59	0.00
Top	-1.39	2.10	0.00
Bridge1	-1.41	2.15	0.00
Bridge2	-1.23	2.17	0.00

**Table 2** Calculated adsorption energies,  $E_{ad}$ , carbon-Pd bond distance  $d_{Pd-C}$ , on different absorption sites on SWNT(10,0),  $d_{Pd-C}$ , and magnetic moment,  $\mu$ .

System	$E_{ad}$ (eV)	$d_{Pd-C}$ (Å)	$\mu$ ( $\mu_B$ )
Hollow	-1.44	2.93	0.00
Top	-1.44	2.14	0.00
Bridge1	-1.33	2.17	0.00
Bridge2	-1.45	2.14	0.00

The calculated adsorption energy for SWNT(6,6) and (10,0) are listed in Table 1 and 2. The adsorption energies of Pd atoms on four different sites ranges from  $\sim -1$  to  $\sim -1.4$  eV. The average Pd-tube bond length occurs in the range of 2.1-2.6 Å. The Pd atom is found to be energetically most favorable to bridge 1 site on (6,6) tube, with a bond distance of 2.15 Å, and bridge 2 site on (10,0) tube, with a bond distance of 2.14 Å. Comparing the adsorption energy of all site, the hollow site is obviously unstable for Pd atom adsorption on a (6,6) tube. Other

three sites on (10,0) tube are about equally favorable for Pd atom adsorption. The binding energies of Pd atom on (6,6) tube is relatively smaller than (10,0) tube due to the smaller curvature of the first one.

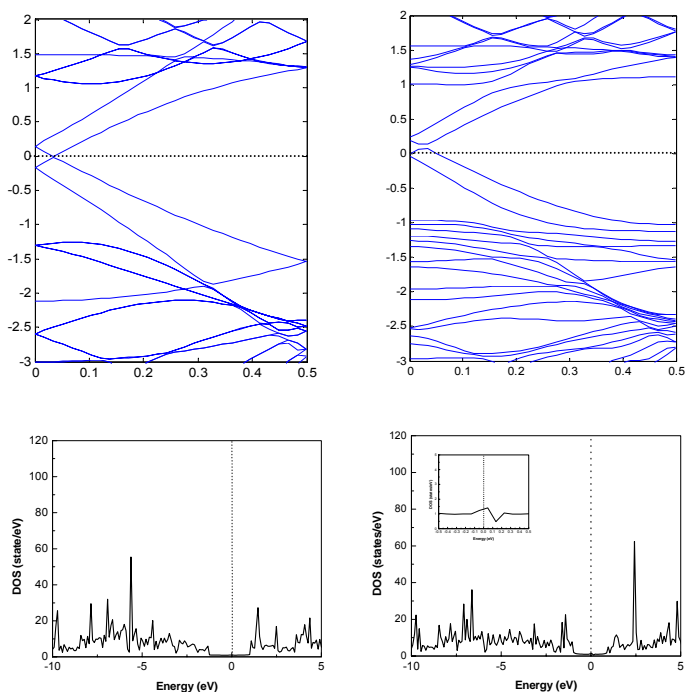


Fig 2 Band structure of clear (right) SWNT(6,6) and (left) single Pd atom adsorbed SWNT(6,6), calculated for the three primitive unit cells consisting of 72 carbon atoms. The Fermi level energy is set to 0 eV.

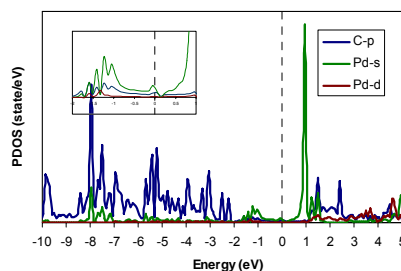


Fig. 3 PDOS from s and d orbitals of Pd atom, and p orbital of two nearest C atom on the b1 site.

The electronic structures of the bare (6,6) tube affected by Pd atom adsorption on a bridge 1 site are shown in Fig. 2. The bare (6,6) SWNT is metallic, therefore the  $\pi$ - $\pi^*$  bands degenerate at the Fermi level as shown in the left part of Fig.2. The modification of electronic structure is induced by the adsorption of a Pd atom. The degeneracy of  $\pi$ - $\pi^*$  bands of clear (6,6) tube at the Fermi level is removed and a gap of  $\sim 80$  meV appears upon the adsorption of Pd. Such opening of a small gap has also been reported by the electronic calculations of metallic chain adsorbed on metallic SWNTs,<sup>31,32</sup> and occurs mainly because of broken symmetry. However the metallic character of the system remains upon the Pd adsorption, because Pd produces a slightly upward shift of valence band, generating a doubly occupied band on the Fermi level. The overall total DOS near Fermi level appears to be similar to that of the bare tube, except that the nearly constant DOS around  $E_f$  have a slight increase of 35%, followed by a 48% decrease to a minimum value of 0.04 states/eV·cell. This is the consequence of a reduced symmetry explained by Delenay<sup>33</sup>, as also shown in the case of Au atom adsorption on (6,6) tube.<sup>34</sup> As can be seen from projected density of states (PDOS) in fig.3, the flat bands at  $\sim -1.0$  eV consist of 5s orbitals, and the conduction bands at  $\sim 1.0$  eV and  $\sim 2.5$  eV contain contributions from 5s and 4d anti-bonding orbital respectively.

The Pd-C bonding state around  $\sim -1$  eV has a major contribution from Pd s orbitals and C p orbitals. This is because despite  $4d^{10}5s^0$  electronic structure of Pd has the lowest ground

state energy, Pd usually shows the reactivity characteristic for a transition metal, where open-shell configuration  $4d^95s^1$  is seen. Charge transfer study shows there is only 0.14 electrons transferred from Pd to the (6,6) tube. For the case of adsorption of Pd on a (10,0) tube, we can see bands (Fig.4) from Pd are inserted at almost the same place in the band structure plot as that of the (6,6) tube, and the original bands from bare tubes are perturbed. Also similar as the Pd+(6,6) tube system, the crossed or almost degenerated states in the (10,0) tube are split in both valance and conduction bands due to the perturbation by the Pd atom, which reduces the symmetry of the wave function in the tube. The band gap between the conduction and valance bands of the (10,0) tube has decreased from 0.75eV to 0.6eV, and the top of valance band stays right below the Fermi level at the  $\Gamma$  point ( $k=0$ ). The existence of the gap above Fermi level still keeps the (10,0) tube semiconducting, even though it has been reduced. We believe that if more Pd atoms are adsorbed, it will further reduce the gap and finally turn the (10,0) tube metallic. This hypothesis was proven in our studies of a Pd chain on the same tube, where the band gap is closed upon a Pd chain adsorption. We observed a charge transfer of  $0.22 e^-$  from Pd atom to the (10,0) tube. The larger charge transfer on the SWNT(10,0) than the SWNT(6,6) is consistent with their adsorption energy differences. The charge density contour plots calculated on a plane passing through the Pd atom and its nearest two carbon atoms are presented in Fig. 5(a), and PDOS is presented in Fig.5(b). We noticed that the bridge 2 site C atoms of (10,0) tube has a stronger bonding states with Pd than the (6,6) tube. This can be seen from a better overlap between C p orbital and Pd d orbital at 0.5~-1eV below Fermi level.

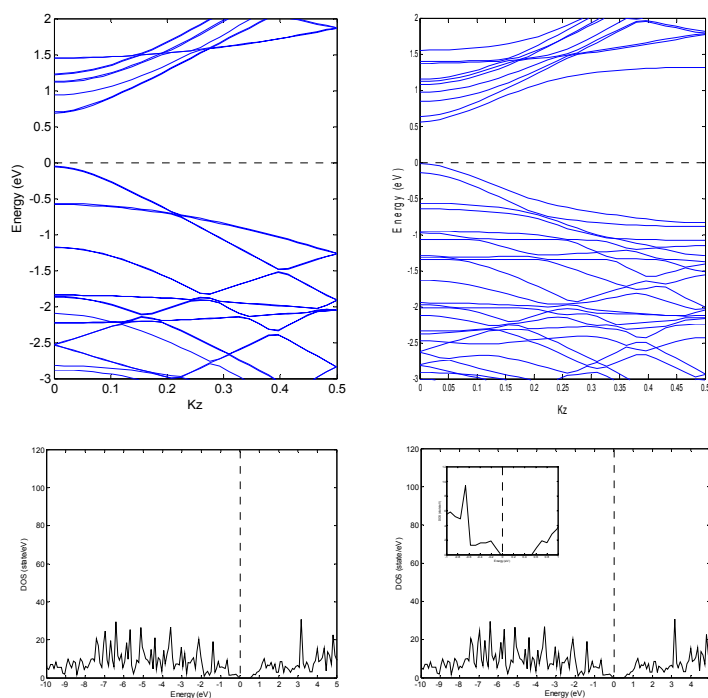


Fig. 4 Band structure of clear (right) SWNT(6,6) and (left) single Pd atom adsorbed SWNT(10,0), calculated for the three primitive unit cells consisting of 80 carbon atoms. The Fermi level energy is set to 0 eV

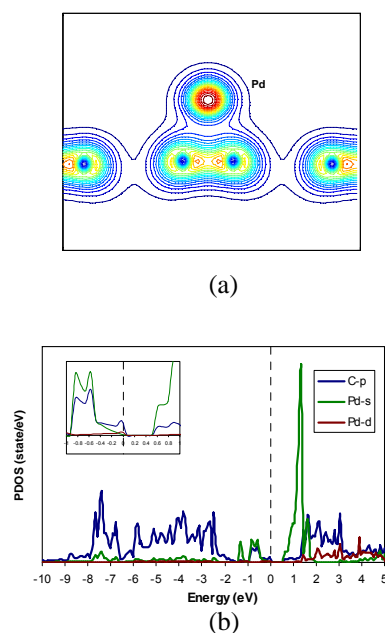


Fig. 5 (a) Counter plot of total charge density of Pd on the bridge 2 site of SWNT(10,0) surface. (b) PDOS from s and d orbitals of Pd atom, and p orbital of two nearest C atoms under the b2 site.

## B. Hydrogen atom interactions with Pd functionalized SWNTs

The adsorption of Hydrogen atom induced a significant modification in the bands of Pd functionalized SWNTs. We first performed H atom on the Pd+(6,6) system, with Pd and C atoms fixed. As can be seen in the Fig.6, the flat half filled 1s bands occur in the different places of the valence band. 1s( $\uparrow$ ) appears  $\sim 0.5\text{eV}$  below  $E_F$ , while 1s( $\downarrow$ ) appears on the Fermi surface. The highest occupied spin-up and lowest empty spin-down band has a minute gap of  $\sim 0.02\text{eV}$ . The position of the new hydrogen band indicates whether the associated localized state is a donor or acceptor state. It is obvious that the one hydrogen band is occupied with one electron, while the unoccupied occurs on the Fermi level, indicating that the H atom tends to attract electrons from Pd and SWNT(6,6) system. Projected density of states (PDOS) shows the new bands are from bonding  $\pi$ - $\sigma$  and anti-bonding  $\pi^*$ - $\sigma^*$  orbitals. The equilibrium PH bond length on SWNT(6,6) is calculated as  $1.62 \text{ \AA}$ . We also calculated PdH bond with respect to free Pd and H atoms. The result of  $1.54 \text{ \AA}$  is consistent with both the experimental data ( $1.53 \text{ \AA}$ ),<sup>35</sup> and the theoretical calculation.<sup>36</sup> Therefore PdH on SWNT(6,6) has a longer bond length than that of the free molecule due to the interaction between Pd and the tube.

The electronic structure and nature of the PdH bond was extensively studied during the 70-80s.<sup>37,38,39</sup> It is well known that the lowest state that can lead to the formation of a stable bond with H arises from the  $4d^9 5s^1$  configuration. However, despite the singly occupied valence s being available to form a single two-electron bond with 1s from H atom, the participation of the 4d electrons from Pd has significant contribution in the Pd-H bonding. From PDOS plots, we can clearly see that the outer s electron on the Pd is primarily responsible for the Pd-H bonding at  $\sim 0.5\text{eV}$  below Fermi level, but the hybridizations of the Pd d orbitals with the s orbital from H is not negligible. On the other hand, we did not observe overlaps between Pd s and C p orbitals around  $\sim -1\text{eV}$  as shown in the previous case without hydrogen (Fig.3), instead we see a good match of s orbital from H with the p orbitals from C between  $-1\sim -3\text{eV}$ . Most interactions between Pd and C atoms is primarily due to the overlap of Pd-s orbital and C-p orbitals below  $-3\text{eV}$ , where they simultaneously interact with s orbital from H. Contour plot of total charge density in Fig.7(a) shows the nature of bonding among H, Pd and C atoms. The spin density in Fig.7(b) indicates large positive spin density is at Pd atom, showing like a d orbital shape, and at H atom showing as s orbital shape, while some negative spin density appears in the interstitial region between Pd and H. This indicates that the influence of magnetic moment ( $0.7 \mu_B$  as calculated) is concentrated on Pd and H atoms, and not on C atoms.

We did not observe large electron overlaps between C and Pd atoms, therefore Pd-C is a weak bond compared to Pd-H bond. The binding energy of a single Hydrogen atom on the (6,6) tube supported Pd is calculated as  $1.60\text{eV}$ , which is lower than that of  $2.34\text{eV}$  of the PdH molecule with respect to the free Pd and H atoms on the CASSCF and MRSDCI levels<sup>39</sup>, and  $2.43 \text{ eV}$  at the GGA level<sup>40</sup>. Therefore the adsorption of H atom weakened by SWNT(6,6), but still within the energy range of chemisorption. A charge of  $0.34 e^-$  was observed to be transferred to the H antibonding state from the Pd functionalized (6,6) tube. This number is higher than a maxima  $0.3 e^-$  charge transfer from Pd to H in the PdH system, based on APW calculations.<sup>41</sup> We assign this effect to the existence of carbon nanotube, because unlike gaining charge previously from Pd without H, the previous excess charges plus extra  $0.04 e^-$  on the tube are actually transferred back to the PdH complex this time, therefore extra charge transfer is observed and some holes might be seen on the (6,6) tube.

The effect of H adsorption on Pd functionalized SWNT(10,0) is still under investigation, more results will be reported later.

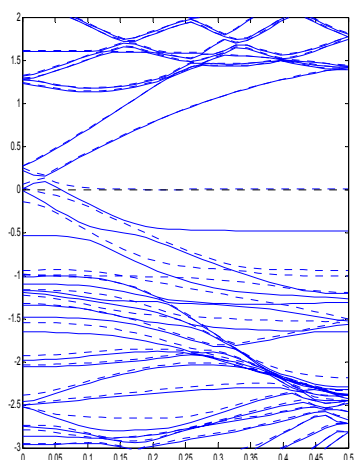


Fig 6 Band structure of Hydrogen adsorbed Pd-SWNT(6,6) The Fermi level energy is set to 0 eV. Spin-up and spin-down states are shown by solid and dotted lines respectively.

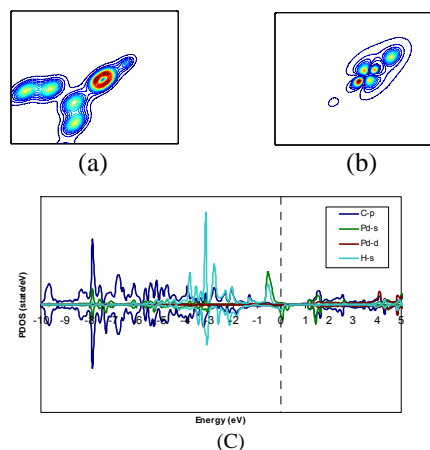


Fig. 7. Contour plot of (a) total charge density and (b) magnetization density on a plane perpendicular to the tube axis and passing through Pd and H atoms on SWNT(6,6). (c) spin polarized PDOS contributed from Pd, H, and two nearest carbon atoms

### C. Hydrogen molecule interactions with Pd functionalized SWNTs

The Palladium atom can also bind two hydrogen atoms in the gas phase. The dihydrogen complex of H<sub>2</sub> and Pd was reported to have an H-H bond length of 0.86 Å, and a Pd-H bond length of 1.67 Å.<sup>42</sup> In investigating the adsorption of a H<sub>2</sub> molecule on SWNT(6,6) supported Pd, we do observe the significant increase of the H-H bond, where the distance between the two H atoms are 0.84 Å. The Pd-H bond length is observed as 1.76 Å. We calculated the total energy difference between the initial Pd-SWNT(6,6) and H<sub>2</sub> state and the final H<sub>2</sub>-Pd-SWNT(6,6) state, in order to calculate the binding energy for this dissociative adsorption. We obtained the result of -0.79 eV. This association energy of is much higher than the physisorption of H<sub>2</sub> on bare SWNTs. The system is nonmagnetic once the hydrogen is attached to Pd, therefore spin polarized calculation is not necessary.

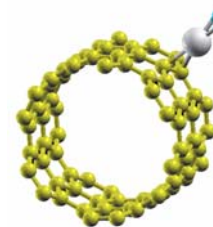


Fig.8 dissociation of H<sub>2</sub> molecule on Pd

The effect of Hydrogen molecule adsorption on Pd functionalized SWNT(10,0) is still under investigation.

### Acknowledgement

The authors thank Dr. Martin M. Ossowski for some valuable discussions. We also would like to thank the Academic Computing at University of South Florida for providing computational resources.

---

\*Corresponding author email: Venkat@eng.usf.edu

- 1 S. Iijima, *Nature* (London) **354**, 56 (1991).
- 2 P. J. F. Harris *Carbon Nanotubes and Related Structures* Cambridge University Press, Cambridge, 1999.
- 3 R. Saito, G. Dresselhaus, and M. S. Dresselhaus, *Physical Properties of Carbon Nanotubes* Imperial College Press, London, 1998.
- 4 A. Modi, N. Koratkar, E. Lass, B. Wei, and P. M. Ajayan, *Nature*, **424**, 171 (2003).
- 5 Y. M. Wong, W. P. Kang, J. L. Davidson, A. Wisitsora-at, and K. L. Soh, *Sens. Actuators B* **93**, 327 (2003).
- 6 O. K. Varghese, *et al.* *Sens. Actuator B* **81**, 32 (2001).
- 7 Y. X. Liang, Y. J. Chen, and T. H. Wang, *Appl. Phys. Lett.* **85**, 666 (2004).
- 8 P. G. Collins, K. Bradley, M. Ishigami, A. Zettl, *Science* **287**, 1801 (2000).
- 9 S. Chopra, K. McGuire, N. Gothard, A. M. Rao, and P. Pham, *Appl. Phys. Lett.* **83**, 2280 (2003).
- 10 J. Kong, *et al.* *Science* **287**, 622 (2000).
- 11 J. Li, *et al.* *Nano Lett.* **3**, 929 (2003).
- 12 J. P. Novak, *et al.* *Appl. Phys. Lett.* **83**, 4026 (2003).
- 13 T. Someya, J. Small, P. Kim, C. Nuckolls, and J. T. Yardley, *Nano Lett.* **3**, 877 (2003).
- 14 A. Star, J-C. P. Gabriel, K. Bradley, and G. Gründer, *Nano Lett.* **3**, 459 (2003).
- 15 K. Bradley, M. Briman, A. Star, and G. Gründer, *Nano Lett.* **4**, 253 (2004).
- 16 S. Peng, and K Cho *Nano Lett.* **3**, 513 (2003).
- 17 J. Kong, M. G. Chapline, and H. Dai, *Adv. Mater.* **13**, 1384 (2001).
- 18 Y. Lu, *et al.* *Chem. Phys. Lett.* **391**, 344 (2004).
- 19 E. Bekyarova, *et al.* *J. Phys. Chem. B* **108**, 19717 (2004).
- 20 B-Y. Wei, *et al.* *Sens. Actuators*, **101**, 81 (2004).
- 21 P. Qi, *et al.* *Nano Lett.* **3**, 347 (2003).
- 22 A. Star, T-R. Han, V. Joshi, J-C. P. Gabriel, and George Gründer, *Adv. Matter.* **16**, 2049 (2004).
- 23 H. S. Nalwa (Editor) *Encyclopedia of Nanoscience and Nanotechnology X*, American Scientific Publishers (2004)
- 24 S. Iijima and T. Ichihashi, *Nature*, **363**, 603 (1993).
- 25 G. Kressee and J. Hafner, *Phys. Rev. B* **47**, 558 (1993); *ibid.* **49**, 14251 (1994).
- 26 G. Kresse, and J. Furthmüller, *Comput. Mat. Sci.* **6**, 15 (1996).
- 27 G. Kresse and J. Furthmüller, *Phys. Rev. B* **54**, 11169 (1996).
- 28 J. P. Perdew and Y. Wang, *Phys. Rev. B* **46**, 6671 (1992).
- 29 H. J. Monkhorst and J. D. Pack, *Phys. Rev. B* **13**, 5188 (1976).
- 30 E. Durgun E. Durgun, S. Dag, V. M. K. Bagci, O. Gülseren, T. Yildirim, and S. Ciraci, *Phys. Rev. B* **67**, 201401(R) (2002).
- 31 K. Kong, S. Han, and J. Ihm, *Phys. Rev. B* **60**, 6074 (1999).
- 32 C. K. Yang, J. Zhao, and J. P. Lu, *Phys. Rev. B* **66**, 041403(R) (2002).
- 33 P. Delaney, H. J. Choi, J. Ihm, S. G. Louie, and M. L. Cohen, *Nature* **391**, 466 (1998).
- 34 E. Durgun, S. Dag, S. Ciraci, and O. Gülseren, *J. Phys. Chem.* **108**, 575 (2004).
- 35 C. Malmberg, R. Scullman, and P. Nylen, *Ark. Fys.* **39**, 495 (1969).
- 36 K. Balasubramanian, *J. Chem. Phys.* **93** 8061 (1990).
- 37 H. Basch, D. Cohen, and S. Topiol, *Isr. J. Chem.* **19**, 233 (1980).
- 38 S. R. Langhoff, L. G. M. Pettersson, C. W. Bauschlicher, Jr., and H. Patridge, Jr, *and. Chem. Phys.* **86**, 268 (1987).
- 39 K. Balasubramanian, *J. Chem. Phys.* **93**, 8061 (1990).
- 40 J. F. Paul, and P. Sautet, *Phys. Rev. B* **53** 8015 (1996).
- 41 D. A. Papaconstantopoulos, B. M. Klein, E. N. Economou, and L. L. Boyer, *Phys. Rev. B* **17**, 141 (1978)
- 42 K. Balasubramanian, P. Y. Feng, and M. Z. Liao, *J. Chem. Phys.* **88**, 6955 (1988).